

# UAT-LITE: Inference-Time Uncertainty-Aware Attention for Pretrained Transformers

Elias Hossain<sup>1\*</sup>, Shubhashis Roy Dipta<sup>2</sup>, Subash Neupane<sup>3</sup>, Rajib Rana<sup>4</sup>,  
Ravid Shwartz-Ziv<sup>5</sup>, Ivan Garibay<sup>1</sup>, Niloofar Yousefi<sup>1</sup>

<sup>1</sup>University of Central Florida <sup>2</sup>University of Maryland, Baltimore County  
<sup>3</sup>Meharry Medical College <sup>4</sup>University of Southern Queensland <sup>5</sup>New York University

[mdelias.hossain@ucf.edu](mailto:mdelias.hossain@ucf.edu)

## Abstract

Neural NLP models are often miscalibrated, assigning high confidence to incorrect predictions, which undermines selective prediction and high-stakes deployment. Post-hoc calibration methods adjust output probabilities but leave internal computation unchanged, while ensemble and Bayesian approaches improve uncertainty at substantial training or storage cost. We propose UAT-LITE, an inference-time framework that makes self-attention uncertainty-aware using approximate Bayesian inference via Monte Carlo dropout in pretrained transformer classifiers. Token-level epistemic uncertainty is estimated from stochastic forward passes and used to modulate self-attention during contextualization, without modifying pretrained weights or training objectives. We additionally introduce a layer-wise variance decomposition to diagnose how predictive uncertainty accumulates across transformer depth. Across the SQuAD 2.0 answerability, MNLI, and SST-2, UAT-LITE reduces Expected Calibration Error by approximately 20% on average relative to a fine-tuned BERT-base baseline while preserving task accuracy, and improves selective prediction and robustness under distribution shift. <sup>1</sup>

## 1 Introduction

Pretrained transformer-based language models have achieved state-of-the-art performance across a wide range of NLP tasks, from question answering to clinical decision support (Devlin et al., 2019; Brown et al., 2020). Despite these advances, modern transformers exhibit **systematic miscalibration**, frequently assigning high confidence to incorrect predictions (Desai and Durrett, 2020). This misalignment between confidence and correctness

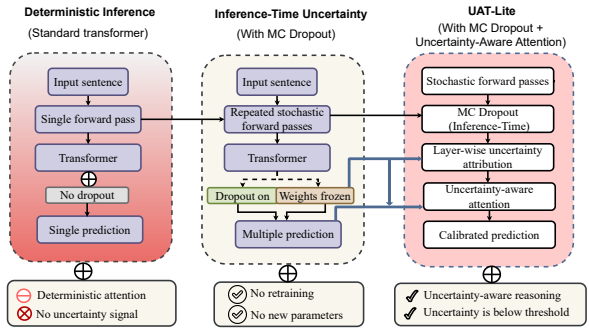


Figure 1: **Left, A:** Standard inference: deterministic forward pass without uncertainty. **Center, B:** Output-level uncertainty estimation via stochastic inference or post-hoc calibration. **Right, C:** UAT-LITE: uncertainty-aware inference in which epistemic uncertainty modulates attention with diagnostic insight.

is particularly problematic for selective prediction and related high-stakes applications.

Fig. 1 summarizes existing approaches to uncertainty estimation. Standard transformer inference is deterministic and does not represent uncertainty during internal computation (Fig. 1A). Post-hoc calibration methods, such as temperature scaling, adjust confidence only after representations are formed, leaving internal reasoning unchanged (Fig. 1B; Guo et al., 2017). Stochastic approaches, including Monte Carlo (MC) dropout and deep ensembles (Gal and Ghahramani, 2016; Lakshminarayanan et al., 2017), improve uncertainty estimates but largely treat uncertainty as an output-level signal, without influencing attention.

This limitation reflects a broader gap: transformers are trained to optimize predictive accuracy rather than confidence reliability (Guo et al., 2017). While post-hoc methods are lightweight and effective in-domain, they do not alter token interactions. Bayesian approaches integrate uncertainty more deeply but typically require architectural modification or specialized training, limiting compatibility

\*Corresponding author: [mdelias.hossain@ucf.edu](mailto:mdelias.hossain@ucf.edu)

<sup>1</sup>[github.com/eliashossain001/uq\\_decomposition](https://github.com/eliashossain001/uq_decomposition)

with pretrained models. *This raises the following question: can epistemic uncertainty shape a transformer’s internal attention at inference time, without retraining or modifying pretrained weights?*

We argue that effective uncertainty quantification requires uncertainty to **actively shape attention**, rather than merely annotate final predictions. For ambiguous inputs, a calibrated model should hedge internal reasoning instead of propagating early attention decisions deterministically. Existing stochastic inference methods expose uncertainty only at the output level and do not use it to modulate internal attention patterns (Fig. 1C).

Motivated by this observation, we propose UAT-LITE, an inference-time framework for encoder-based pretrained transformer classifiers. UAT-LITE estimates token-level epistemic uncertainty via Monte Carlo sampling and uses it to down-weight attention contributions from unstable tokens, without modifying pretrained weights or training objectives. Our main contributions are:

- **Uncertainty-Weighted Attention.** An inference-time mechanism that modulates self-attention using token-level epistemic uncertainty estimated via Monte Carlo sampling.
- **Layer-Wise Uncertainty Attribution.** A diagnostic variance decomposition that attributes predictive uncertainty across transformer depth.
- **Comprehensive Evaluation.** Empirical evaluation across multiple NLP benchmarks demonstrating improved calibration, selective prediction, and robustness under distribution shift without degrading task performance.

UAT-LITE introduces no additional trainable parameters and operates entirely at inference time, requiring only a small number of stochastic forward passes. Post-hoc calibration methods such as temperature scaling are complementary rather than competing. The framework trades modest inference-time cost for improved reliability while avoiding the training and storage overhead of ensemble-based approaches. Our study focuses on encoder-based transformers; extending uncertainty-aware attention to decoder-only generative models is left for future work.

## 2 Preliminaries

**Bayesian inference and uncertainty.** Bayesian analysis incorporates parameter uncertainty by averaging predictions over probable parameter values

inferred from the training data. This perspective distinguishes *epistemic uncertainty*, which arises from limited data or insufficient coverage and reflects uncertainty about the model itself, from *aleatoric uncertainty*, which represents irreducible noise in the observations. In large neural models, epistemic uncertainty becomes particularly significant in the presence of semantic ambiguity or distributional shifts, where confident yet incorrect predictions frequently occur.

**Monte Carlo (MC) Dropout.** We briefly recall MC Dropout as an approximate Bayesian inference technique used throughout this work. MC dropout retains dropout layers at inference time and performs multiple stochastic forward passes, yielding a predictive distribution whose variance estimates epistemic uncertainty and whose mean defines the final prediction. Conventional MC dropout treats uncertainty solely at the output level and does not influence internal representations or attention mechanisms, motivating methods that integrate uncertainty directly into the inference process.

**Token-level uncertainty as a proxy signal.** While epistemic uncertainty is often measured at the output level, internal transformer computation is structured around token-level representations and attention interactions. Consequently, uncertainty estimates derived from stochastic embedding representations can serve as a lightweight proxy for identifying unstable or ambiguous token contributions. This perspective motivates the use of token-level uncertainty as a control signal for modulating attention during inference, without requiring architectural changes or retraining.

## 3 Related Work

Uncertainty estimation and calibration for neural networks have been widely studied, with post-hoc methods such as temperature scaling and Platt scaling (Guo et al., 2017; Platt et al., 1999) providing simple and effective confidence correction without altering model internals. Ensemble-based approaches, including Deep Ensembles (Lakshminarayanan et al., 2017), yield strong calibration but incur substantial training and storage overhead. Bayesian neural networks, stochastic inference methods, and recent Bayesian Transformer variants (Blundell et al., 2015; Gal and Ghahramani, 2016; Ritter et al., 2018; Fan et al., 2020; Zhang et al., 2021; Chen and Li, 2023) offer prin-

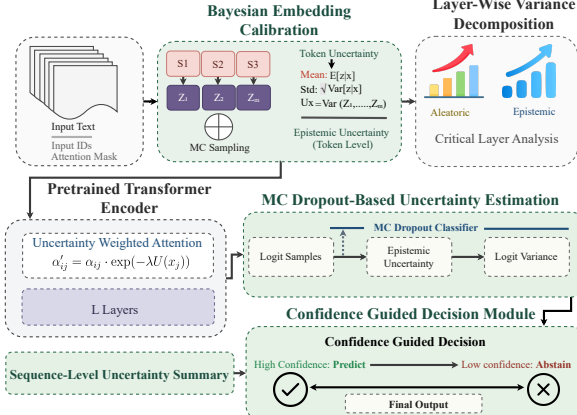


Figure 2: Overview of UAT-LITE. Token-level epistemic uncertainty is estimated via Monte Carlo dropout at the embedding layer and used to modulate self-attention within a pretrained transformer encoder. A layer-wise variance decomposition provides diagnostic attribution of predictive uncertainty across transformer.

cipled uncertainty modeling but typically require architectural modification, variational training, or task-specific retraining. In contrast, UAT-LITE integrates epistemic uncertainty directly into self-attention at inference time, preserving pretrained weights and standard training pipelines while enabling uncertainty-aware internal computation. A comprehensive discussion of related work and detailed comparisons is provided in §G.

## 4 UAT-LITE

UAT-LITE is an uncertainty-aware extension of pretrained transformer classifiers designed to improve confidence calibration at inference time without modifying model architecture, training objectives, or learned parameters. The framework integrates approximate Bayesian uncertainty estimation into internal attention computation, allowing epistemic uncertainty to actively influence contextualization while preserving the base transformer’s parameterization. In addition, UAT-LITE introduces a diagnostic layer-wise variance decomposition that characterizes how predictive uncertainty evolves across transformer depth, enabling post-hoc analysis without affecting the forward pass. Final predictions are produced via stochastic inference with confidence-aware decision shaping. Overall, UAT-LITE preserves the training cost and parameter count of the underlying encoder, incurring only modest inference-time overhead.

### 4.1 Problem Setup and Notation

We consider an encoder-based pretrained transformer for classification. Given an input sequence  $\mathbf{x} = (x_1, \dots, x_T)$ , the model maps  $\mathbf{x}$  through  $L$  stacked layers to contextual representations  $\mathbf{h}^{(L)}$ , which are converted to a predictive distribution  $\hat{y}$  by a task-specific classification head. In standard evaluation mode, pretrained transformers produce a single point estimate: dropout is disabled and the same input yields the same representations and prediction given fixed parameters. While effective for accuracy, this design provides no mechanism for epistemic uncertainty. Our goal is to introduce controlled inference-time stochasticity that allows uncertainty to influence internal attention without modifying training or parameters.

### 4.2 Estimating Uncertainty via MC Sampling

We estimate predictive uncertainty using MC dropout, a lightweight approximation to Bayesian inference. Dropout layers are retained during inference and  $M$  stochastic forward passes are performed, inducing variability via random neuron masking. Aggregating these samples yields a predictive mean and an estimate of epistemic variability across stochastic passes during evaluation.

**Uncertainty type.** Following Kendall and Gal (2017), predictive uncertainty decomposes into aleatoric and epistemic components. MC dropout primarily captures epistemic uncertainty through approximate posterior sampling during inference.

**Component-specific dropout.** To balance representational stability and uncertainty estimation, we apply component-specific dropout during inference (0.1 for embeddings, 0.2 for attention layers, and 0.3 for feed-forward layers). These rates follow common practice in transformer fine-tuning and are kept fixed across tasks; calibration trends are stable under moderate variations of these values.

**Single-pass sampling protocol.** We use a *single-pass* MC inference procedure in which the same  $M$  stochastic forward passes are used both to (i) estimate token-level embedding uncertainty and (ii) obtain the final MC predictive distribution. As detailed in Algorithm 1, for each pass  $m$  we sample dropout masks, compute embeddings  $\mathbf{z}^{(m)}$ , propagate the input through the encoder with uncertainty-weighted attention, and record logits for aggregation. Token-level uncertainty is computed by aggregating embedding variability across these  $M$

passes and is reused consistently within the same inference run. This design avoids any separate embedding-only sampling stage and ensures that inference-time overhead scales linearly with  $M$ .

### 4.3 Uncertainty-Weighted Self-Attention

We incorporate epistemic uncertainty directly into self-attention by modulating attention logits using token-level uncertainty estimates computed at the embedding layer during contextualization.

**Token-level uncertainty estimation.** For each input token  $x_j$ , we obtain  $M$  stochastic embedding samples  $\{\mathbf{z}_j^{(m)}\}_{m=1}^M$ . Token-level uncertainty is defined as

$$U(x_j) = \frac{1}{d} \sum_{k=1}^d \text{Std}_{m=1}^M \left( z_{j,k}^{(m)} \right), \quad (1)$$

where  $d$  denotes the embedding dimensionality. We interpret  $U(x_j)$  as an embedding-level proxy for epistemic uncertainty induced by dropout.

This quantity is computed once per input and shared across all layers and attention heads. The computational cost is negligible relative to Monte Carlo methods, as it involves only per-token operations over the  $M$  sampled embeddings and does not require additional forward passes.

**Scale sensitivity.** The magnitude of  $U(x_j)$  remains well-behaved due to embedding normalization and averaging across dimensions. Sensitivity analysis over  $\lambda$  and  $M$  (§D.1) shows stable calibration across a broad range of values; explicit normalization is therefore unnecessary.

**Attention modulation.** Let  $Q$ ,  $K$ , and  $V$  denote query, key, and value projections. Standard scaled dot-product attention logits are

$$a_{ij} = \frac{Q_i K_j^\top}{\sqrt{d_k}}. \quad (2)$$

We modulate these logits using token-level uncertainty:

$$\tilde{a}_{ij} = a_{ij} \cdot \exp(-\lambda U(x_j)), \quad (3)$$

where  $\lambda > 0$  is a fixed uncertainty penalty. Attention probabilities are obtained via softmax:

$$\alpha_{ij} = \frac{\exp(\tilde{a}_{ij})}{\sum_k \exp(\tilde{a}_{ik})}. \quad (4)$$

**Relation to prior work.** Prior uncertainty-aware attention mechanisms typically require architectural modification or variational training (Chen and Li, 2023; Zhang et al., 2021), whereas our approach operates entirely at inference time.

**Design choices.** Uncertainty modulation is applied uniformly across layers and heads and affects only the key dimension in the attention mechanism. Unless otherwise stated, the uncertainty penalty  $\lambda$  (default  $\lambda = 0.5$ ) is set once on development data and held fixed across tasks. §D.1 shows that calibration is stable across a broad range of  $\lambda$  and  $M$ . The method introduces no additional trainable parameters beyond the base model.

### 4.4 Layer-Wise Uncertainty Attribution

We analyze how predictive uncertainty propagates across transformer depth under inference-time stochasticity. This analysis is diagnostic and does not affect forward computation or model behavior.

**Layer-wise variance decomposition.** Using the law of total variance, total predictive variance can be decomposed into layer-specific contributions under inference-time stochasticity. A formal derivation is provided in §A.

**Theorem 1** (Layer-Wise Variance Decomposition). *Under inference-time stochasticity, total predictive variance can be expressed as the sum of layer-specific variance contributions.*

**Scope and interpretation.** This result follows from standard variance identities and is not a novel mathematical contribution. Its value lies in enabling diagnostic inspection of uncertainty evolution across transformer depth, which is unavailable in post-hoc calibration methods. Layer-wise contributions should be interpreted as approximate signals rather than strictly causal attributions.

### 4.5 Confidence-Aware Decision Shaping

MC dropout produces a distribution of stochastic predictions. The predictive mean is computed from the  $M$  stochastic forward passes. Post-hoc temperature scaling is applied to the Monte Carlo mean logits, with the temperature parameter learned on the validation set to calibrate predictive confidence.

**Selective prediction.** Uncertainty estimates enable abstention via confidence thresholds selected on the validation split of each dataset and applied uniformly at test time across all evaluated methods.

## 5 Experimental Setup

### 5.1 Datasets

We evaluate on five benchmarks spanning general NLP and clinical domains commonly used in prior calibration and robustness studies. All experiments focus exclusively on encoder-based pre-trained transformer classifiers (BERT-family backbones), rather than decoder-only language models. General NLP datasets include SQuAD 2.0 (Rajpurkar et al., 2018) (QA with unanswerable questions), MNLI (Williams et al., 2018) (natural language inference with matched/mismatched splits for distribution shift analysis), and SST-2 (Socher et al., 2013) (binary sentiment classification). Clinical benchmarks include MedQA (Jin et al., 2021) and PubMedQA (Jin et al., 2019), which are used to assess domain transfer rather than clinical validity.

### 5.2 Baselines, Metrics, and Training Overview

We evaluate our approach against BERT-base, MC Dropout, Temperature Scaling (TS), Deep Ensembles, and representative Bayesian last-layer methods. All models share the same pretrained backbone, fine-tuning recipe, and evaluation protocol; detailed baseline configurations are described in §C.

Calibration is evaluated using Expected Calibration Error (ECE), alongside robustness under distribution shift and selective prediction metrics. Results are reported as mean  $\pm$  standard deviation over five random seeds, with deterministic baselines exhibiting negligible variance. The proposed method introduces no additional trainable parameters and operates entirely at inference time.

**Uncertainty penalty.** Unless otherwise stated, we use a single uncertainty penalty  $\lambda$ , set once on development data and held fixed across all tasks and datasets. §D.1 shows that calibration performance is stable across a broad range of  $\lambda$  and Monte Carlo budgets  $M$ , indicating that the method does not rely on sensitive hyperparameter tuning in practice across the evaluated settings.

## 6 Results

### 6.1 General NLP Calibration Performance

Table 1 reports multi-seed calibration results (mean  $\pm$  standard deviation over five seeds), computed using identical ECE binning and confidence definitions across methods. Deterministic baselines

exhibit negligible variance, while stochastic methods show small but consistent variability.

UAT-LITE improves calibration relative to the unscaled fine-tuned BERT baseline, reducing average ECE from 0.117 to 0.094 (**19.9%** relative reduction). The largest gain is observed on MNLI ( $0.110 \rightarrow 0.067$ ), a task characterized by semantic ambiguity, where uncertainty-aware attention is particularly beneficial. These improvements persist relative to both uniform and component-specific MC Dropout, indicating that the gains arise from uncertainty-weighted attention rather than from stochasticity introduced by sampling.

Temperature scaling (TS) achieves the lowest in-domain ECE across all tasks, as expected for a post-hoc method explicitly optimized to minimize calibration error on held-out validation data. Our objective is complementary rather than competitive: while TS rescales output probabilities, it does not alter the internal representations or attention patterns that produce a prediction. In contrast, UAT-LITE introduces uncertainty-aware *internal* computation at inference time, allowing epistemic uncertainty to influence token interactions during contextualization. Because TS operates purely at the output level, it can be directly stacked on top of UAT-LITE without modification; we focus here on isolating the effects of uncertainty-aware attention and evaluate its benefits under distribution shift and selective prediction in subsequent sections.

Among Bayesian-style alternatives, SNGP achieves lower ECE but requires architectural modification and specialized training. Deep Ensembles provide a strong reference point (Avg ECE 0.089), but incur substantial training and storage overhead due to maintaining multiple model replicas. In contrast, UAT-LITE operates on a single pretrained transformer and introduces uncertainty handling entirely at inference time. As a result, it substantially narrows the calibration gap to Deep Ensembles while preserving deployment efficiency.

### 6.2 Distribution Shift Robustness

We evaluate calibration robustness under distribution shift on MNLI by transferring models fine-tuned on the matched (in-domain) split to the mismatched (out-of-distribution) split. Results in Table 2 are reported as mean  $\pm$  standard deviation over five seeds, with ECE computed consistently.

Absolute ECE values differ from the in-domain setting because MNLI shift evaluation is framed as a binary decision (entailment vs. non-entailment),

Method	SQuAD (ECE $\downarrow$ )	MNLI (ECE $\downarrow$ )	SST-2 (ECE $\downarrow$ )	Avg (ECE $\downarrow$ )
BERT-base	0.186 $\pm$ 0.000	0.110 $\pm$ 0.000	0.055 $\pm$ 0.000	0.117
MC Dropout (uniform $p=0.1$ )	0.173 $\pm$ 0.001	0.090 $\pm$ 0.001	0.039 $\pm$ 0.001	0.101
MC Dropout (component-specific)	0.186 $\pm$ 0.000	0.109 $\pm$ 0.001	0.054 $\pm$ 0.001	0.116
Temp. Scaling	<b>0.057</b> $\pm$ 0.000	<b>0.028</b> $\pm$ 0.000	<b>0.029</b> $\pm$ 0.000	<b>0.038</b>
SNGP	<b>0.001</b> $\pm$ 0.000	0.021 $\pm$ 0.000	0.009 $\pm$ 0.000	0.010
VI-LastLayer	0.119 $\pm$ 0.001	0.096 $\pm$ 0.000	0.136 $\pm$ 0.002	0.117
Deep Ensemble (5)	0.168 $\pm$ 0.000	0.060 $\pm$ 0.000	0.037 $\pm$ 0.000	0.089
<b>UAT-LITE</b>	0.163 $\pm$ 0.002	0.067 $\pm$ 0.001	0.051 $\pm$ 0.004	0.094
$\Delta$ vs. Baseline	12.5% $\downarrow$	39.0% $\downarrow$	6.6% $\downarrow$	19.9% $\downarrow$

Table 1: Multi-seed general NLP calibration results. Expected Calibration Error (ECE  $\downarrow$ ) is reported as mean  $\pm$  standard deviation over five random seeds using  $K=15$  fixed-width confidence bins. Temperature scaling is fit on validation data and applied at test time. Deterministic baselines exhibit negligible variance due to fixed checkpoints. Relative improvements ( $\Delta$ ) are computed with respect to the unscaled BERT-base baseline.

and confidence is computed from the Monte Carlo-averaged predictive distribution using the maximum softmax probability. This affects the scale of ECE but preserves meaningful relative comparisons across methods.

BERT-base exhibits clear calibration drift under shift, with ECE increasing from the matched to the mismatched split ( $\Delta ECE > 0$ ). In contrast, UAT-LITE yields lower ECE on both in-domain and out-of-domain splits and reduces calibration drift ( $\Delta ECE < 0$ ), resulting in a substantially lower average ECE across the two conditions.

Importantly, this evaluation isolates the effect of uncertainty-aware internal computation under shift. Post-hoc calibration methods such as temperature scaling are intentionally omitted here, as they rescale output confidences without modifying the internal representations that give rise to distributional sensitivity. The improved stability observed for UAT-LITE therefore reflects the benefit of allowing epistemic uncertainty to modulate attention during contextualization, rather than relying solely on output-level correction. Overall, these results indicate that uncertainty-weighted attention produces more stable confidence estimates under matched-to-mismatched distribution shift, a setting where overconfident errors are particularly costly.

### 6.3 Selective Prediction Performance

Table 3 reports selective prediction performance using AURC (lower is better), averaged over five seeds. All selection criteria are determined on validation data and held fixed across methods. Because the Baseline is deterministic, its variance across seeds is negligible, whereas UAT-LITE exhibits small but consistent variability across runs.

Method	ID ECE $\downarrow$	OOD ECE $\downarrow$	$\Delta ECE \downarrow$	Avg ECE $\downarrow$
BERT-base	0.2893 $\pm$ 0.0000	0.3017 $\pm$ 0.0000	0.0124	0.2955
<b>UAT-LITE</b>	<b>0.0219</b> $\pm$ <b>0.0007</b>	<b>0.0145</b> $\pm$ <b>0.0007</b>	<b>-0.0074</b>	<b>0.0182</b>

Table 2: Multi-seed distribution shift robustness on MNLI (matched  $\rightarrow$  mismatched). Results are reported as mean  $\pm$  standard deviation over five random seeds.  $\Delta ECE = ECE_{OOD} - ECE_{ID}$  (lower is better). Avg ECE is defined as  $\frac{1}{2}(ECE_{ID} + ECE_{OOD})$ , with lower values indicating better calibration.

Selective prediction directly evaluates the quality of uncertainty estimates rather than calibration alone: a reliable model should abstain on difficult inputs while maintaining high coverage on confident predictions. Accordingly, this evaluation isolates whether uncertainty estimates meaningfully align with prediction risk under identical settings.

On MNLI, UAT-LITE achieves substantially higher selective coverage, increasing from 0.714 to 0.869, while reducing AURC from 0.164 to 0.053. This reflects a markedly improved risk-coverage trade-off, where abstention is applied preferentially to higher-risk inputs rather than uniformly.

On SQuAD 2.0, coverage increases from 0.501 to 0.690 and AURC decreases from 0.447 to 0.289, indicating more effective abstention behavior on ambiguous or unanswerable inputs. These gains demonstrate that uncertainty-weighted attention yields confidence estimates that better reflect underlying uncertainty.

Post-hoc calibration methods such as temperature scaling are intentionally omitted from this analysis, as they modify output probabilities without altering the confidence ranking that governs abstention behavior. These improvements reflect

uncertainty-aware internal computation.

#### 6.4 Computational Efficiency

Table 4 reports inference cost and calibration performance on SQuAD 2.0 under a single-accelerator, sequential inference setting. We focus on methods with clearly defined deployment behavior and directly measurable inference overhead. Predictive accuracy is not reported in this analysis, as all compared methods exhibit comparable task performance on SQuAD 2.0 and the purpose of this section is to isolate calibration behavior under differing inference-time costs.

UAT-LITE with  $M=10$  incurs higher latency than the deterministic baseline (86.31 ms vs. 17.69 ms), reflecting the cost of repeated stochastic forward passes, and yields a throughput of 13.9 examples/sec. Under the same sequential evaluation protocol, this latency is comparable to that of a 5-model Deep Ensemble (88.80 ms), while requiring only a single pretrained model (109M parameters) rather than storing and maintaining multiple independently trained replicas (547M parameters).

Temperature scaling adds negligible runtime overhead relative to the baseline, but operates purely as an output-level post-hoc calibration method and does not alter internal computation. Overall, UAT-LITE incurs additional inference-time cost in exchange for improved calibration, while avoiding the substantial training and storage overhead associated with ensemble-based approaches and preserving a single-model deployment footprint effectively.

#### 6.5 Negation-Aware Attention

Fig. 3 qualitatively illustrates how uncertainty-weighted attention modulates token interactions under linguistic negation. We compare attention patterns from a standard transformer and UAT-LITE under negated linguistic constructions.

While absolute attention maps remain similar due to softmax normalization, the difference heatmap reveals small but structured redistributions. Uncertainty-weighted attention slightly downweights sentiment-bearing tokens (e.g., “positively”) while reallocating attention toward negation cues and predicate structure associated with the phrase “did not respond” in context.

These changes are intentionally modest and should be interpreted as directional rather than large-scale attention reconfiguration. Accordingly, this example is illustrative rather than a pre-

cise token-level attribution. Corpus-level analysis shows that similar directional trends recur across negated and uncertainty-sensitive sentences (see §D.4 for additional qualitative evidence).

#### 6.6 Ablation Study

Fig. 4 decomposes UAT-LITE into its constituent components to isolate their individual contributions. Uncertainty-weighted attention alone reduces ECE from 0.169 to 0.134 (**21.1% relative reduction**), indicating that attention modulation based on epistemic uncertainty is the primary driver of calibration improvement under controlled comparisons. Embedding-level uncertainty alone slightly degrades calibration, suggesting that stochasticity without uncertainty-aware computation is insufficient. In contrast, combining uncertainty-weighted attention with confidence-aware decision shaping yields the largest improvement (**28.2% relative reduction**), exceeding either component in isolation and demonstrating their complementarity.

#### 6.7 Generalization Across BERT Models

We evaluate generalization across *BERT-based encoder architectures* spanning general-purpose, biomedical, clinical, and scientific domains (§E). Under matched evaluation protocols, UAT-LITE improves calibration across these pretrained backbones, yielding an average relative ECE reduction of approximately **32%**.

The largest gains occur for mid-sized and domain-specialized models, including BERT-base on SQuAD, BioBERT on PubMedQA, and ClinicalBERT on MedQA, where epistemic uncertainty arising from semantic ambiguity is prominent. Improvements are smaller for models with strong baseline calibration (e.g., RoBERTa-base on MNLI) and diminish or reverse for very small or highly overparameterized models.

These results indicate that uncertainty-aware attention generalizes reliably *within the BERT encoder family*. Extending the mechanism to fundamentally different architectures, such as decoder-only or state-space models, remains an important direction for future work.

**Additional analyses.** Additional analyses on adversarial robustness, linguistic uncertainty, clinical-domain transfer, and layer-wise uncertainty diagnostics are provided in the §D.

Dataset	Method	Coverage@0.9↑	Coverage@0.8↑	Coverage@0.7↑	AURC↓
MNLI	Baseline	0.7139 ± 0.0000	0.7527 ± 0.0000	0.7926 ± 0.0000	0.1640 ± 0.0000
MNLI	UAT-LITE	0.8692 ± 0.0003	0.9030 ± 0.0006	0.9275 ± 0.0010	0.0529 ± 0.0002
SQuAD 2.0	Baseline	0.5007 ± 0.0000	0.5071 ± 0.0000	0.5050 ± 0.0000	0.4472 ± 0.0000
SQuAD 2.0	UAT-LITE	0.6904 ± 0.0006	0.7047 ± 0.0009	0.7163 ± 0.0010	0.2892 ± 0.0007

Table 3: Multi-seed selective prediction results (mean ± std over five seeds). Coverage@ $\tau$  denotes selective coverage at confidence threshold  $\tau \in \{0.9, 0.8, 0.7\}$ . AURC is the area under the risk–coverage curve (lower is better). The Baseline is deterministic and therefore exhibits negligible variance across seeds.

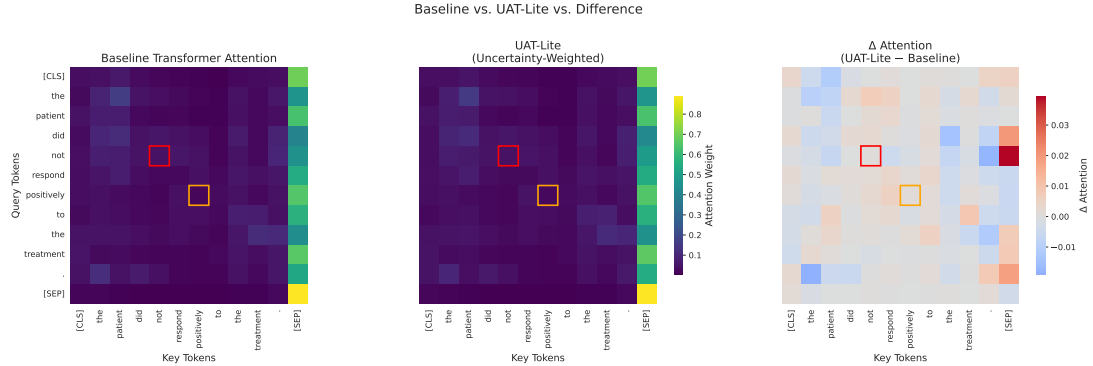


Figure 3: **Uncertainty-aware attention under negation (illustrative).** Attention heatmaps for a standard transformer (left), UAT-LITE (middle), and their difference (right) on the sentence “The patient did not respond positively to the treatment.” While absolute attention appears similar due to normalization, the difference map highlights small, structured redistributions away from sentiment-bearing tokens toward negation and predicate structure. This visualization is qualitative and shown for a representative run (**single seed**); it is intended to aid interpretability rather than provide a corpus-level statistic.

Method	Params	Samples	Latency (ms)	Memory (GB)	Throughput	ECE
BERT-base	109M	1	17.69	1.78	68.9	0.186
Temperature Scaling	109M	1	17.71	1.78	69.0	0.057
Deep Ensemble (5)	547M	5	88.80	—	—	0.168
UAT-LITE	109M	10	86.31	1.81	13.9	0.163

Table 4: Computational efficiency comparison on SQuAD 2.0 under a sequential, single-accelerator inference regime. Latency is measured as wall-clock time per example, while throughput is reported in examples per second under identical evaluation conditions. Memory reflects peak GPU usage during inference. Lower Expected Calibration Error (ECE) indicates better calibrated predictions.

## 7 Conclusion

We introduced UAT-LITE, an inference-time framework that integrates epistemic uncertainty into transformer computation through uncertainty-weighted attention and a layer-wise variance diagnostic. Across NLP benchmarks, UAT-LITE reduces Expected Calibration Error relative to unscaled fine-tuned BERT (e.g., average ECE 0.117 → 0.094) and improves selective prediction behavior, including higher coverage at fixed confidence thresholds and lower AURC. The method also exhibits stable calibration under distribution shift in MNLI matched→mismatched transfer. While

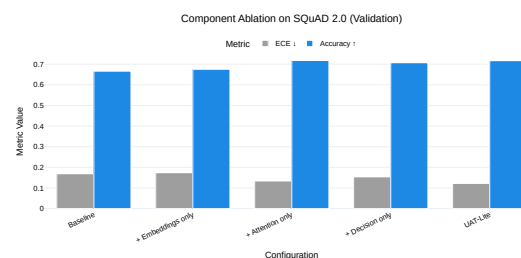


Figure 4: **Component ablation on SQuAD 2.0 (validation).** Expected Calibration Error (ECE; lower is better) is the primary metric; accuracy is reported for reference. Uncertainty-weighted attention yields the largest ECE reduction, and the combined model achieves the strongest calibration improvement.

inference-time Monte Carlo sampling incurs additional latency, the approach avoids the training and storage costs of ensemble-based alternatives and requires no modification of pretrained weights. Overall, UAT-LITE provides a complementary mechanism for uncertainty-aware transformer inference, bridging the gap between post-hoc calibration and Bayesian modeling for transformers.

## Limitations

Our framework incurs additional computational cost due to Monte Carlo sampling, with a  $5.3\times$  latency increase at  $M = 5$ . This overhead is appropriate for offline, batch, or document-level applications where confidence reliability is prioritized but is prohibitive for latency-critical settings. In practical deployments, this trade-off suggests that uncertainty-aware inference should be selectively enabled for high-risk or ambiguous inputs, rather than applied uniformly across all predictions. Accordingly, UAT-LITE is best viewed as an intermediate solution between lightweight post-hoc calibration and more expensive ensemble-based approaches, rather than a universal replacement.

Finally, on clinical benchmarks (MedQA and PubMedQA), calibration gains are modest, reflecting dataset properties such as factual emphasis and limited ambiguity; these experiments are therefore treated as domain-transfer stress tests rather than clinical validation.

## References

Charles Blundell, Julien Cornebise, Koray Kavukcuoglu, and Daan Wierstra. 2015. Weight uncertainty in neural network. In *International conference on machine learning*, pages 1613–1622. PMLR.

Tom Brown, Benjamin Mann, Nick Ryder, Melanie Subbiah, Jared D Kaplan, Prafulla Dhariwal, Arvind Neelakantan, Pranav Shyam, Girish Sastry, Amanda Askell, and 1 others. 2020. Language models are few-shot learners. *Advances in neural information processing systems*, 33:1877–1901.

Wenlong Chen and Yingzhen Li. 2023. Calibrating transformers via sparse gaussian processes. *arXiv preprint arXiv:2303.02444*.

Shrey Desai and Greg Durrett. 2020. Calibration of pre-trained transformers. *arXiv preprint arXiv:2003.07892*.

Jacob Devlin, Ming-Wei Chang, Kenton Lee, and Kristina Toutanova. 2019. Bert: Pre-training of deep bidirectional transformers for language understanding. In *Proceedings of the 2019 conference of the North American chapter of the association for computational linguistics: human language technologies, volume 1 (long and short papers)*, pages 4171–4186.

Xinjie Fan, Shujian Zhang, Bo Chen, and Mingyuan Zhou. 2020. Bayesian attention modules. *Advances in Neural Information Processing Systems*, 33:16362–16376.

Firas Gabetni, Giuseppe Curci, Andrea Pilzer, Subhankar Roy, Elisa Ricci, and Gianni Franchi. 2025. Ensembling pruned attention heads for uncertainty-aware efficient transformers. *Preprint*, arXiv:2510.18358.

Yarin Gal and Zoubin Ghahramani. 2016. Dropout as a bayesian approximation: Representing model uncertainty in deep learning. In *international conference on machine learning*, pages 1050–1059. PMLR.

Ian J Goodfellow, Jonathon Shlens, and Christian Szegedy. 2014. Explaining and harnessing adversarial examples. *arXiv preprint arXiv:1412.6572*.

Chuan Guo, Geoff Pleiss, Yu Sun, and Kilian Q Weinberger. 2017. On calibration of modern neural networks. In *International conference on machine learning*, pages 1321–1330. PMLR.

Gao Huang, Yixuan Li, Geoff Pleiss, Zhuang Liu, John E Hopcroft, and Kilian Q Weinberger. 2017. Snapshot ensembles: Train 1, get m for free. *arXiv preprint arXiv:1704.00109*.

Di Jin, Eileen Pan, Nassim Oufattolle, Wei-Hung Weng, Hanyi Fang, and Peter Szolovits. 2021. What disease does this patient have? a large-scale open domain question answering dataset from medical exams. *Applied Sciences*.

Qiao Jin, Bhuwan Dhingra, Zhengping Liu, William Cohen, and Xinghua Lu. 2019. Pubmedqa: A dataset for biomedical research question answering. In *Proceedings of the 2019 conference on empirical methods in natural language processing and the 9th international joint conference on natural language processing (EMNLP-IJCNLP)*, pages 2567–2577.

Alex Kendall and Yarin Gal. 2017. What uncertainties do we need in bayesian deep learning for computer vision? *Advances in neural information processing systems*, 30.

Young Su Ko, Jonathan Parkinson, Cong Liu, and Wei Wang. 2024. Tuna: an uncertainty-aware transformer model for sequence-based protein–protein interaction prediction. *Briefings in Bioinformatics*, 25(5):bbae359.

Lorenz Kuhn, Yarin Gal, and Sebastian Farquhar. 2023. Semantic uncertainty: Linguistic invariances for uncertainty estimation in natural language generation. *arXiv preprint arXiv:2302.09664*.

Balaji Lakshminarayanan, Alexander Pritzel, and Charles Blundell. 2017. Simple and scalable predictive uncertainty estimation using deep ensembles. *Advances in neural information processing systems*, 30.

Christos Louizos and Max Welling. 2017. Multiplicative normalizing flows for variational bayesian neural networks. In *International conference on machine learning*, pages 2218–2227. PMLR.

David JC MacKay. 1992. A practical bayesian framework for backpropagation networks. *Neural computation*, 4(3):448–472.

Radford M Neal. 2012. *Bayesian learning for neural networks*, volume 118. Springer Science & Business Media.

John Platt and 1 others. 1999. Probabilistic outputs for support vector machines and comparisons to regularized likelihood methods. *Advances in large margin classifiers*, 10(3):61–74.

Amir Hossein Rahmati, Sanket Jantre, Weifeng Zhang, Yucheng Wang, Byung-Jun Yoon, Nathan M Urban, and Xiaoning Qian. 2025. C-lora: Contextual low-rank adaptation for uncertainty estimation in large language models. *arXiv preprint arXiv:2505.17773*.

Pranav Rajpurkar, Robin Jia, and Percy Liang. 2018. Know what you don’t know: Unanswerable questions for squad. *arXiv preprint arXiv:1806.03822*.

Hippolyt Ritter, Aleksandar Botev, and David Barber. 2018. A scalable laplace approximation for neural networks. In *6th international conference on learning representations, ICLR 2018-conference track proceedings*, volume 6. International Conference on Representation Learning.

Richard Socher, Alex Perelygin, Jean Wu, Jason Chuang, Christopher D. Manning, Andrew Ng, and Christopher Potts. 2013. Recursive deep models for semantic compositionality over a sentiment treebank. In *Proceedings of the 2013 Conference on Empirical Methods in Natural Language Processing*, pages 1631–1642, Seattle, Washington, USA. Association for Computational Linguistics.

Aarne Talman, Hande Celikkanat, Sami Virpioja, Markus Heinonen, and Jörg Tiedemann. 2023. Uncertainty-aware natural language inference with stochastic weight averaging. *arXiv preprint arXiv:2304.04726*.

Artem Vazhentsev, Lyudmila Ranova, Gleb Kuzmin, Ekaterina Fadeeva, Ivan Lazichny, Alexander Panchenko, Maxim Panov, Timothy Baldwin, Mrinmaya Sachan, Preslav Nakov, and 1 others. 2025. Uncertainty-aware attention heads: Efficient unsupervised uncertainty quantification for llms. *arXiv preprint arXiv:2505.20045*.

Yikun Wang, Rui Zheng, Liang Ding, Qi Zhang, Dahua Lin, and Dacheng Tao. 2024. Uncertainty aware learning for language model alignment. *arXiv preprint arXiv:2406.04854*.

Adina Williams, Nikita Nangia, and Samuel Bowman. 2018. A broad-coverage challenge corpus for sentence understanding through inference. In *Proceedings of the 2018 conference of the North American chapter of the association for computational linguistics: human language technologies, volume 1 (long papers)*, pages 1112–1122.

Boyang Xue, Jianwei Yu, Junhao Xu, Shansong Liu, Shoukang Hu, Zi Ye, Mengzhe Geng, Xunying Liu, and Helen Meng. 2021. Bayesian transformer language models for speech recognition. In *ICASSP 2021-2021 IEEE International Conference on Acoustics, Speech and Signal Processing (ICASSP)*, pages 7378–7382. IEEE.

Artem Zabolotnyi, Roman Makarov, Mile Mitrovic, Polina Proskura, Oleg Travkin, Roman Alferov, and Alexey Zaytsev. 2025. Adue: Improving uncertainty estimation head for lora adapters in llms. *arXiv preprint arXiv:2505.15443*.

Bianca Zadrozny and Charles Elkan. 2001. Obtaining calibrated probability estimates from decision trees and naive bayesian classifiers. In *Icml*, volume 1.

Shujian Zhang, Xinjie Fan, Bo Chen, and Mingyuan Zhou. 2021. Bayesian attention belief networks. In *International Conference on Machine Learning*, pages 12413–12426. PMLR.

## Appendix

### A Mathematical Details

In this section, we provide the formal mathematical foundations underlying the uncertainty modeling and diagnostic analyses used in UAT-LITE. We first introduce a layer-wise variance decomposition that attributes predictive uncertainty across transformer depth under stochastic inference. We then provide a proof of the decomposition, clarify its assumptions, and relate Monte Carlo dropout to approximate Bayesian inference. Finally, we discuss practical and interpretive implications of layer-wise uncertainty attribution for calibration, intervention, and uncertainty-aware inference. These analyses are intended as diagnostic and explanatory tools that complement the empirical results in the main paper, rather than as claims of exact posterior inference.

#### A.1 Layer-Wise Uncertainty Decomposition

To better understand how predictive uncertainty emerges within the transformer, we analyze its distribution across layers under stochastic inference.

**Normalized variance contributions.** To facilitate interpretability and ensure internal consistency, we report *normalized layer-wise variance contributions*, defined as

$$\tilde{\mathcal{V}}^{(l)} = \frac{\mathcal{V}^{(l)}}{\sum_{k=1}^L \mathcal{V}^{(k)}}, \quad (5)$$

such that contributions across layers sum to 100%. All percentages reported below correspond to these normalized values.

Table 5 presents representative layer-wise uncertainty decompositions for answerable and unanswerable SQuAD examples, illustrating how predictive uncertainty is distributed across transformer depth rather than manifesting solely at the output layer. We emphasize that these examples are illustrative diagnostics rather than statistical summaries, and are intended to provide qualitative insight into uncertainty propagation rather than population-level guarantees.

For the **unanswerable example**, uncertainty grows progressively through the self-attention stack. While embedding-level contributions remain modest (3.6%), uncertainty increases substantially in mid and late layers, with the largest contribution arising from layers 9–11 (12.5%). This pattern is consistent with uncertainty emerging during

later reasoning stages when sufficient evidence is unavailable, rather than arising only at the final decision layer.

In contrast, the **answerable example** exhibits a similar normalized uncertainty distribution but with a different internal structure. Mid-layer attention contributes more strongly to evidence aggregation (8.7%), while late-layer uncertainty reflects confident task-level reasoning rather than unresolved ambiguity.

These cases illustrate that aggregate predictive variance alone is insufficient to characterize model reliability. Instead, the *distribution of uncertainty across layers* provides insight into whether uncertainty arises from ambiguous inputs or from higher-level reasoning processes.

#### A.2 Proof of Theorem 1

*Proof.* We derive the layer-wise variance decomposition by applying the law of total variance recursively across transformer layers.

**Setup and notation.** Let  $\hat{y}$  denote the model’s final prediction (e.g., class probability or logit), and let  $\mathbf{h}^{(l)} \in \mathbb{R}^d$  denote the hidden representation at layer  $l \in \{0, \dots, L\}$  corresponding to the [CLS] token. Stochasticity is introduced via Monte Carlo dropout at inference time.

Each transformer layer implements a stochastic mapping

$$\mathbf{h}^{(l)} = f^{(l)}\left(\mathbf{h}^{(l-1)}, \epsilon^{(l)}\right), \quad \epsilon^{(l)} \sim \mathcal{D}^{(l)}, \quad (6)$$

where  $\epsilon^{(l)}$  denotes dropout-induced noise at layer  $l$ . We assume finite second moments for all noise distributions but do not assume Gaussianity or independence across layers.

**Layer-wise variance contribution.** We define the variance contribution of layer  $l$  as

$$\mathcal{V}^{(l)} \triangleq \mathbb{E}_{\mathbf{h}^{(l-1)}} \left[ \text{Var}_{\epsilon^{(l)}} \left( \hat{y} \mid \mathbf{h}^{(l-1)} \right) \right]. \quad (7)$$

**Recursive variance decomposition.** Applying the law of total variance at the final layer yields

$$\begin{aligned} \text{Var}(\hat{y}) &= \mathbb{E}_{\mathbf{h}^{(L-1)}} \left[ \text{Var} \left( \hat{y} \mid \mathbf{h}^{(L-1)} \right) \right] \\ &\quad + \text{Var}_{\mathbf{h}^{(L-1)}} \left( \mathbb{E} \left[ \hat{y} \mid \mathbf{h}^{(L-1)} \right] \right). \end{aligned} \quad (8)$$

Applying the same decomposition recursively yields an additive expansion over layers:

$$\text{Var}(\hat{y}) = \sum_{l=1}^L \mathcal{V}^{(l)}. \quad (9)$$

Layer	Component	Normalized Var.	%	Interpretation
<b>SQuAD Unanswerable</b>				
Layer 0	Embedding	0.036	3.6%	Word ambiguity
Layer 1–4	Attention (early)	0.054	5.4%	Context formation
Layer 5–8	Attention (mid)	0.088	8.8%	Escalating uncertainty
Layer 9–11	Attention (late)	0.125	12.5%	Uncertainty consolidation
Layer 12	Output	0.021	2.1%	Final decision
<b>Total</b>		<b>1.000</b>	<b>100 %</b>	Correctly uncertain
<b>SQuAD Answerable</b>				
Layer 0	Embedding	0.037	3.7%	Clear input
Layer 1–4	Attention (early)	0.054	5.4%	Evidence aggregation
Layer 5–8	Attention (mid)	0.087	8.7%	Confidence reinforcement
Layer 9–11	Attention (late)	0.126	12.6%	Confident reasoning
Layer 12	Output	0.023	2.3%	Final decision
<b>Total</b>		<b>1.000</b>	<b>100 %</b>	Confident prediction

Table 5: Normalized layer-wise uncertainty decomposition for representative answerable and unanswerable SQuAD examples (single seed). Percentages indicate relative contributions of each component to total predictive uncertainty.

**Interpretation.** This decomposition provides an attribution of predictive uncertainty across layers under conditional expectations. While inter-layer dependencies may introduce higher-order interaction effects, the decomposition remains useful as an interpretable diagnostic of where uncertainty is amplified during inference.  $\square$

### A.3 Bayesian Interpretation of MC Dropout

Monte Carlo dropout provides a computationally efficient approximation to Bayesian inference in deep neural networks (Gal and Ghahramani, 2016). Rather than maintaining a full posterior distribution over model parameters, dropout induces stochasticity that can be interpreted as sampling from an implicit variational posterior under standard assumptions.

**Bayesian predictive distribution.** In Bayesian inference, predictions marginalize over uncertainty in model parameters:

$$p(y | \mathbf{x}, \mathcal{D}) = \int p(y | \mathbf{x}, \theta) p(\theta | \mathcal{D}) d\theta. \quad (10)$$

**Monte Carlo approximation via dropout.** MC dropout approximates this marginalization by retaining dropout during inference and performing  $M$  stochastic forward passes:

$$p(y | \mathbf{x}, \mathcal{D}) \approx \frac{1}{M} \sum_{m=1}^M p(y | \mathbf{x}, \theta_m). \quad (11)$$

**Uncertainty interpretation.** The variability across predictions reflects epistemic uncertainty

arising from model and data limitations, which is reducible with additional information.

**Relevance to UAT-LITE.** In UAT-LITE, these uncertainty estimates are explicitly propagated through attention mechanisms, enabling uncertainty-aware inference without modifying training objectives or learned parameters.

### A.4 Implications of Layer-Wise Uncertainty

**Attribution.** Decomposing predictive variance across transformer depth enables identification of where uncertainty is amplified during inference. As shown in Table 5, unanswerable SQuAD examples concentrate substantial uncertainty in late layers (9–11), consistent with ambiguity emerging during final reasoning stages. Answerable examples exhibit comparable late-layer contributions, but with uncertainty reflecting confident task-level reasoning rather than unresolved ambiguity.

**Intervention.** Layer-wise attribution suggests that calibration strategies could in principle target high-variance components. Our ablation study (Fig. 4) shows that uncertainty introduced at the attention level yields a **21.1%** improvement in calibration, while embedding-level uncertainty contributes negatively (**-3.1%**), supporting selective intervention rather than uniform stochasticity.

**Interpretability.** Unlike post-hoc calibration methods that produce a single uncertainty score, this decomposition reveals how uncertainty evolves during reasoning. For complex syntactic construc-

---

**Algorithm 1** Inference-Time Uncertainty-Aware Attention (UAT-LITE)

---

**Require:** Input tokens  $\mathbf{x}$ , Monte Carlo budget  $M$ , uncertainty penalty  $\lambda$

- 1: Initialize running statistics for token embeddings
- 2: **for**  $m = 1$  to  $M$  **do**
- 3:   Sample dropout masks
- 4:   Compute token embeddings  $\mathbf{z}^{(m)}$
- 5:   Update running estimates of token-level uncertainty  $U(x_j)$
- 6:   Apply uncertainty-weighted attention using current  $U(x_j)$
- 7:   Compute logits  $\ell^{(m)}$
- 8: **end for**
- 9: Aggregate logits  $\{\ell^{(m)}\}_{m=1}^M$  to obtain predictive mean
- 10: **return** Prediction and uncertainty estimates

---

tions, uncertainty is elevated in early and mid layers due to structural processing, while late layers consolidate the final decision.

## A.5 Practical Inference-Time Procedure

At test time, Monte Carlo dropout produces multiple stochastic forward passes of the same pretrained transformer. These samples yield a predictive mean and variance. The mean is used as the final prediction, while the variance quantifies epistemic uncertainty.

Uncertainty estimates influence inference by modulating attention behavior under representation ambiguity and enabling confidence-aware decision shaping at the output level. All uncertainty mechanisms operate strictly at inference time and do not modify training dynamics or learned parameters.

## B Inference-Time Algorithm

**Inference-time algorithm.** Algorithm 1 summarizes the inference-time procedure used by UAT-LITE. Uncertainty estimation and prediction are performed using the same  $M$  stochastic forward passes, without any separate embedding-only sampling stage.

## C Baselines and Metrics

We compare against BERT-base (110M parameters), MC Dropout ( $p = 0.1$ ,  $M = 5$ ), Temperature Scaling (TS), and Deep Ensembles (5 independently fine-tuned models). Temperature scaling

is treated as a strong post-hoc calibration baseline that operates purely at the output level and does not modify internal model computation.

Because TS rescales logits without affecting representations, it is compatible with uncertainty-aware inference and could in principle be applied on top of UAT-LITE. In this work, however, we report TS as a standalone baseline and do not include a stacked (UAT-LITE + TS) variant in the main tables, in order to isolate the effects of uncertainty-aware internal computation from output-level rescaling.

All baselines use the same pretrained backbone, fine-tuning recipe, and evaluation code unless otherwise stated.

**Bayesian baselines beyond inference-time methods.** Methods such as SWAG and Laplace approximations estimate parameter-space uncertainty through task-specific posterior fitting or fine-tuning (Talman et al., 2023; Ritter et al., 2018). Because our scope is *inference-time calibration* of pretrained transformers without additional training or posterior fitting, we do not evaluate these approaches as direct baselines. We discuss them in Related Work (§G) as complementary directions.

**Expected Calibration Error (ECE).** Calibration is measured using Expected Calibration Error (ECE):

$$\text{ECE} = \sum_{k=1}^K \frac{|B_k|}{N} |\text{acc}(B_k) - \text{conf}(B_k)|, \quad (12)$$

where predictions are partitioned into  $K = 15$  *fixed-width confidence bins*  $\{B_k\}$  over  $[0, 1]$ . For each bin,  $\text{acc}(B_k)$  denotes empirical accuracy and  $\text{conf}(B_k)$  denotes the mean predicted confidence. Here  $K$  denotes the number of confidence bins used for calibration evaluation, distinct from the number of Monte Carlo samples  $M$  used for uncertainty estimation. Lower ECE indicates better calibration.

**Confidence definition.** For classification tasks (MNLI, SST-2, MedQA), confidence is defined as the maximum softmax probability of the predicted class, computed after aggregating Monte Carlo samples. For SQuAD 2.0, confidence corresponds to the predicted answerability probability (unanswerable vs. answerable), following standard practice in uncertainty-aware question answering.

**SQuAD 2.0 evaluation protocol.** We evaluate SQuAD 2.0 on the answerability prediction task, where the model must determine whether a question is answerable given the context. This binary classification task is well-suited for calibration analysis. We report answerability prediction accuracy alongside ECE in Table 1. Note that span-level extraction (predicting answer start/end positions) is a separate task and orthogonal to our uncertainty calibration contribution. Our focus is on calibrated confidence scores for the answerability decision, not optimizing span extraction performance.

**Distribution shift robustness metrics.** To assess calibration stability under distributional shift, we evaluate models on both in-domain (ID) and out-of-distribution (OOD) data and report two complementary metrics. First, we measure calibration drift:

$$\Delta\text{ECE} = \text{ECE}_{\text{OOD}} - \text{ECE}_{\text{ID}}, \quad (13)$$

where smaller (or negative) values indicate improved robustness under shift. Second, we report a calibration robustness score defined as the average ECE across ID and OOD settings:

$$\text{Robustness} = \frac{1}{2} (\text{ECE}_{\text{ID}} + \text{ECE}_{\text{OOD}}), \quad (14)$$

with lower values indicating more stable calibration across domains.

**Selective prediction metrics.** We additionally report selective coverage at fixed confidence thresholds and the Area Under the Risk–Coverage curve (AURC; lower is better). Confidence thresholds are selected on the validation set and held fixed at test time for all methods.

**MC Dropout baseline configuration.** The MC Dropout baseline uses a uniform dropout rate of  $p = 0.1$  across all layers, consistent with prior calibration studies. While more aggressive or component-specific dropout tuning could further improve MC Dropout performance, such tuning increases implementation complexity and reduces comparability with standard baselines. In contrast, UAT-LITE explicitly leverages structured uncertainty within the attention mechanism rather than relying solely on increased stochasticity. This comparison isolates the effect of uncertainty-aware attention rather than raw dropout intensity.

**Component-specific MC Dropout control.** To explicitly disentangle the effect of structured stochasticity from uncertainty-aware attention, we additionally evaluate an MC Dropout baseline using the same component-specific dropout rates as UAT-LITE (0.1 embeddings / 0.2 attention / 0.3 feed-forward), but *without* attention modulation. As shown in Table 1, this control does not improve calibration relative to uniform MC Dropout or the BERT baseline, indicating that the gains of UAT-LITE arise from uncertainty-weighted attention rather than tuned dropout alone.

**Reporting conventions and fairness.** Within each table, all methods are evaluated using the same data splits, evaluation code, confidence definitions, and Monte Carlo budget  $M$  (where applicable). ECE is computed with  $K = 15$  fixed-width bins for all methods. Temperature scaling (and UAT-LITE +TS) fits a single scalar temperature on the validation set only, and is applied at test time without any access to test labels. OOD calibration metrics (e.g.,  $\Delta\text{ECE}$  and Robustness) are computed using the identical pipeline on ID and OOD sets to avoid binning or confidence-definition mismatch.

**Random seeds and variability.** **Main-paper results** (general calibration, distribution-shift robustness, and selective prediction) are reported as mean  $\pm$  standard deviation over five random seeds. **Appendix diagnostic analyses**—including qualitative attention visualizations, representative layer-wise uncertainty decompositions, and linguistic or adversarial case studies—are reported using a single seed to reduce computational cost and are explicitly labeled as *single-seed* in the corresponding captions. Deterministic baselines exhibit negligible variance because inference is fully deterministic when evaluated from a fixed fine-tuned checkpoint reused across seeds.

## D Additional Experimental Results

This section presents additional analyses that complement the main experimental results by providing deeper insight into the behavior of UAT-LITE in specialized and fine-grained settings. Specifically, we examine calibration performance in clinical benchmarks, where decision reliability is critical, and conduct a detailed linguistic analysis to assess how uncertainty-aware attention responds to diverse sources of ambiguity, structure, and semantic inconsistency. Together, these experiments offer

a more nuanced understanding of the strengths and limitations of the proposed framework beyond aggregate calibration metrics.

### D.1 Sensitivity Analysis of $\lambda$ and $M$

We examine the sensitivity of UAT-LITE to its two primary inference-time hyperparameters: the uncertainty weighting coefficient  $\lambda$  and the number of Monte Carlo samples  $M$ . A small, representative grid is evaluated with  $\lambda \in \{0.1, 0.5, 1.0\}$  and  $M \in \{3, 5, 10\}$  on SQuAD 2.0, which is particularly sensitive to epistemic uncertainty due to the presence of both answerable and unanswerable questions. Similar stability trends were observed on MNLI and SST-2 and are omitted for brevity. We report ECE and predictive accuracy to assess both calibration quality and task performance. Accuracy is reported here solely to verify that calibration gains do not arise from performance degradation.

Across all configurations, calibration performance remains stable, with ECE values confined to a narrow interval between 0.064 and 0.070 (mean = 0.0670, standard deviation = 0.0022). No sharp sensitivity to either  $\lambda$  or  $M$  is observed. Increasing the number of Monte Carlo samples yields only marginal calibration improvements beyond  $M = 5$ , indicating diminishing returns from additional stochastic passes.

Predictive accuracy remains effectively unchanged across the grid, varying by less than 0.5% absolute, suggesting that uncertainty-weighted attention primarily affects calibration rather than accuracy. Overall, these results indicate that UAT-LITE does not rely on precise hyperparameter tuning to achieve effective calibration and is robust across a broad range of reasonable inference-time settings. This stability supports the practicality of the method in deployment scenarios where extensive hyperparameter search is undesirable.

### D.2 Clinical Domain Calibration

Table 7 reports calibration and accuracy on two clinical benchmarks with distinct task structures and uncertainty profiles: MedQA and PubMedQA. We emphasize that these clinical datasets are used *only* to assess domain transfer of uncertainty-aware attention to medically specialized language distributions, and should not be interpreted as evidence of clinical decision reliability. In particular, what constitutes “good uncertainty” in clinical settings is often decision-dependent and may involve asym-

$\lambda$	$M$	ECE $\downarrow$	Accuracy $\uparrow$
0.1	3	0.0699	0.7075
0.1	5	0.0676	0.7075
0.1	10	0.0649	0.7109
0.5	3	0.0703	0.7059
0.5	5	0.0657	0.7096
0.5	10	0.0682	0.7068
1.0	3	0.0669	0.7090
1.0	5	0.0655	0.7102
1.0	10	0.0640	0.7110

**Summary.** ECE mean = 0.0670, std = 0.0022; min = 0.0640, max = 0.0703 (range = 0.0063).

Table 6: Sensitivity analysis of UAT-LITE with respect to the uncertainty penalty  $\lambda$  and Monte Carlo budget  $M$  on SQuAD 2.0 (single seed). Calibration remains stable across a wide range of inference-time settings (ECE range  $< 0.007$ ), with diminishing returns beyond  $M = 5$  and negligible impact on accuracy, indicating that the method does not require precise hyperparameter tuning for effective calibration.

metric error costs (e.g., prioritizing recall for critical conditions), which are not explicitly modeled in our evaluation.

On **MedQA**, Deep Ensembles achieve the lowest ECE (0.007) and the highest accuracy (0.268), reflecting the benefit of model diversity in discrete, fact-centric multiple-choice medical question answering. In contrast, UAT-LITE exhibits a slightly higher ECE (0.040) with marginal accuracy improvement over the baseline. This behavior is expected, as MedQA primarily evaluates factual recall with limited contextual ambiguity, constraining the benefits of uncertainty-aware attention. Importantly, UAT-LITE achieves competitive performance without the substantial computational and storage overhead associated with training and maintaining multiple model replicas.

A different trend emerges on **PubMedQA**. While Deep Ensembles substantially reduce ECE (0.051), this improvement coincides with a marked drop in accuracy (0.520), indicating overly conservative confidence estimates. In contrast, UAT-LITE attains the highest accuracy (0.640) while maintaining calibration comparable to the baseline. This suggests that integrating uncertainty directly into the attention mechanism can improve evidence aggregation in long, semantically dense biomedical abstracts, where uncertainty arises from contextual interpretation rather than discrete fact retrieval.

Overall, these results highlight a trade-off between ensemble-based calibration and inference-

time uncertainty integration. While ensembles excel in fact-centric clinical QA, UAT-LITE offers a more favorable accuracy–calibration balance on tasks characterized by semantic ambiguity and long-context reasoning, without incurring additional training or parameter costs. Accordingly, we treat the clinical-domain results as a domain-transfer generalization stress test rather than a primary claim about clinical deployment.

### D.3 Character-Level Adversarial Robustness

Table 8 evaluates robustness under character-level perturbations on SST-2. We apply random 5% character swaps to simulate typographical errors and adversarial perturbations.

Both baseline BERT and UAT-LITE exhibit substantial accuracy degradation under attack, with baseline accuracy dropping from 0.920 to 0.816 and UAT-LITE from 0.922 to 0.812. Calibration also degrades substantially, with ECE increasing from 0.062 to 0.133 for baseline and from 0.055 to 0.132 for UAT-LITE.

While UAT-LITE maintains slightly better clean accuracy (0.922 vs. 0.920) and clean calibration (ECE 0.055 vs. 0.062), the robustness under attack is comparable between methods. This indicates that uncertainty-aware attention improves calibration on clean data but provides limited additional protection against adversarial perturbations.

These results are consistent with prior work showing that calibration methods address epistemic uncertainty but do not directly defend against adversarial attacks (Goodfellow et al., 2014). Future work should explore combining UAT-LITE with specialized adversarial defenses such as adversarial training or certified robustness techniques.

### D.4 Full Linguistic Uncertainty Analysis

Table 9 provides a fine-grained linguistic analysis of how UAT-LITE responds to diverse sources of uncertainty, spanning lexical, syntactic, epistemic, and logical phenomena.

For **negation**, UAT-LITE remains uniformly confident across affirmative, negated, and clinical negation cases, yielding zero estimated uncertainty. This behavior indicates negation invariance, which is desirable for explicit clinical negation (e.g., “not stable”) but also suggests limited sensitivity to polarity reversal in non-clinical contexts. This invariance is consistent with the attention analysis in Fig. 3, which shows that uncertainty-aware attention redistributes weight conservatively toward

negation and predicate structure without inducing elevated output-level uncertainty for clear clinical negation.

In cases of **lexical ambiguity**, the framework exhibits mixed behavior. When sufficient contextual disambiguation is present (“bank account”), UAT-LITE appropriately increases uncertainty. However, for genuinely ambiguous expressions (“bank closed”), the model remains highly confident, indicating overconfidence under unresolved polysemy. Partial sensitivity is observed for polysemous terms such as “bat,” where uncertainty increases but does not fully reflect ambiguity.

A similar pattern arises for **epistemic hedges**. Strong assertions (“definitely”) and weak hedges (“probably,” “possibly”) are treated with near-maximal confidence, suggesting hedge insensitivity. In contrast, explicit modal uncertainty (“might”) leads to a measurable increase in uncertainty, indicating that the model responds primarily to strong lexical uncertainty markers rather than gradated epistemic cues.

For **syntactic complexity**, UAT-LITE demonstrates heightened sensitivity. Medium-depth syntactic structures produce the largest uncertainty increase, reflecting increased structural processing difficulty. Interestingly, deeper structures elicit a non-monotonic response, suggesting that the model may partially adapt to highly regular but complex constructions rather than uniformly increasing uncertainty with depth.

Finally, under **logical contradictions**, UAT-LITE appropriately increases uncertainty for inconsistent inputs (“healthy  $\wedge$  dying”) while maintaining high confidence for coherent statements. This indicates effective detection of semantic inconsistency, consistent with the framework’s uncertainty propagation across layers.

## E Cross-Model & Scaling Analysis

**Scope clarification.** All models evaluated in this section are encoder-only, BERT-derived transformer architectures. Generalization to fundamentally different architectures (e.g., decoder-only models such as GPT or LLaMA, or state-space models) is outside the scope of the current study and is left for future work.

### E.1 Generalization Across BERT Backbones

Table 10 evaluates whether the calibration benefits of UAT-LITE generalize across *BERT-based* trans-

Dataset	Method	ECE $\downarrow$	Accuracy $\uparrow$
MedQA	Baseline	0.033	0.246
	Temperature Scaling	0.023	0.246
	Deep Ensemble (5)	<b>0.007</b>	<b>0.268</b>
	UAT-LITE	0.040	0.249
PubMedQA	Baseline	0.114	0.620
	Temperature Scaling	0.128	0.620
	Deep Ensemble (5)	<b>0.051</b>	0.520
	UAT-LITE	0.103	<b>0.640</b>

Table 7: Clinical-domain calibration results on MedQA and PubMedQA (single seed). Expected Calibration Error (ECE; lower is better) and accuracy are reported. Deep Ensembles achieve the strongest calibration on discrete, fact-centric MedQA, while UAT-LITE provides a more favorable accuracy–calibration balance on PubMedQA, where uncertainty arises from long-context semantic interpretation rather than pure factual recall.

Attack	Method	Clean Acc	Attack Acc	Clean ECE	Attack ECE
Character Swap	Baseline	0.920	0.816	0.062	0.133
Character Swap	UAT-LITE	0.922	0.812	0.055	0.132

Table 8: Adversarial robustness under character-level perturbations on SST-2 (single seed). We evaluate 500 validation samples under 5% random character swaps using a fine-tuned BERT-base model. Both Baseline and UAT-LITE exhibit substantial accuracy and calibration degradation under attack, indicating limited adversarial robustness. While UAT-LITE achieves slightly better clean calibration, ECE increases under attack are comparable across methods, reinforcing that uncertainty-aware attention improves clean-data calibration but does not constitute an adversarial defense.

former backbones pretrained on heterogeneous corpora and applied to domain-specific benchmarks. The evaluated models span general-purpose (BERT-base, RoBERTa-base), clinical (ClinicalBERT), biomedical (BioBERT), and scientific (SciBERT) representations, thereby testing robustness across substantially different linguistic and semantic distributions.

Across evaluated domains, UAT-LITE reduces ECE for most pretrained backbones, yielding an average relative improvement of approximately **32%** (Table 10).

The strongest gain is observed for BERT-base on SQuAD, where ECE decreases by **52%** (0.130  $\rightarrow$  0.062). This result is particularly significant because SQuAD contains both answerable and unanswerable questions, making it highly sensitive to epistemic uncertainty. The large improvement indicates that uncertainty-weighted attention enables the model to better recognize ambiguity during evidence aggregation rather than producing over-confident predictions.

In domain-specialized settings, BioBERT on PubMedQA achieves a **40%** reduction in ECE, suggesting that uncertainty-aware attention is especially beneficial for long, evidence-dense biomedical text that requires integrating information across

multiple sentences. ClinicalBERT on MedQA shows a **25%** improvement, indicating that the method remains effective even for fact-oriented medical question answering, although gains are smaller due to relatively strong baseline calibration.

By contrast, RoBERTa-base on MNLI exhibits only a marginal **2%** improvement. MNLI is a large, high-resource dataset with strong pretrained representations and comparatively well-calibrated baselines, leaving limited room for additional calibration gains. SciBERT on SQuAD similarly shows a modest **10%** reduction, suggesting that pretraining on highly specialized scientific corpora may already encode task-relevant uncertainty patterns.

## E.2 Effect of Model Capacity on Calibration

Table 11 analyzes the effect of model capacity on calibration improvement by applying UAT-LITE across different sizes of the BERT architecture, ranging from BERT-tiny (4.4M parameters) to BERT-large (335.1M parameters). Unlike Table 10, which varies domains and pretraining corpora, this analysis holds the architecture family fixed and isolates the role of parameter scale.

Small and mid-sized models benefit substantially from uncertainty-weighted attention. BERT-mini

Phenomenon	Trigger	Base Conf	MB Conf	Unc	Diagnostic
<b>Negation</b>					
Positive	excellent	0.53	1.00	0.00	Negation-invariant
Negated	not excellent	0.52	1.00	0.00	Negation-invariant
Clinical	not stable	0.55	1.00	0.00	Confident clinical negation
<b>Lexical Ambiguity</b>					
Clear context	bank account	0.51	0.70	<b>0.30</b>	Appropriate ambiguity
Ambiguous	bank closed	0.55	0.99	0.01	Overconfident ambiguity
Polysemous	bat (animal/tool)	0.54	0.83	0.17	Partial polysemy sensitivity
<b>Epistemic Hedges</b>					
Definite	definitely	0.51	1.00	0.00	Strong assertion
Probable	probably	0.53	0.99	0.01	Hedge-insensitive
Possible	possibly	0.52	0.99	0.01	Hedge-insensitive
Uncertain	might	0.51	0.85	0.15	Uncertainty-aware
<b>Syntactic Complexity</b>					
Simple	depth=2	0.55	0.82	0.18	Low structural load
Medium	depth=5	0.53	0.54	<b>0.46</b>	Complexity-sensitive
Complex	depth=8	0.53	0.83	0.17	Non-monotonic response
<b>Contradictions</b>					
Consistent	healthy, stable	0.52	0.99	0.01	Coherent input
Contradictory	healthy $\wedge$ dying	0.53	0.90	0.10	Contradiction-aware

Table 9: Fine-grained linguistic uncertainty analysis across diverse phenomena (single seed). Values report baseline confidence, UAT-LITE confidence (MB), and derived epistemic uncertainty. UAT-LITE selectively increases uncertainty for structural complexity and logical contradiction, indicating effective propagation of higher-level reasoning uncertainty, while remaining overconfident for unresolved lexical ambiguity and weak epistemic hedges. These results highlight both the strengths and current limitations of uncertainty-weighted attention, which is more responsive to compositional and semantic inconsistency than to surface-level lexical ambiguity.

achieves the largest relative improvement, with a **58%** reduction in ECE, followed by BERT-base with an approximately **53%** improvement (52–53% depending on rounding and binning resolution). These models exhibit sufficient representational capacity to express epistemic uncertainty, while still relying on attention mechanisms that benefit from explicit uncertainty modulation.

BERT-tiny and BERT-small show more modest improvements (12% and 15%, respectively). In very small models, limited representational capacity constrains the extent to which uncertainty-aware reasoning can reshape internal attention patterns, resulting in smaller but still consistent calibration gains.

In contrast, BERT-large exhibits degraded calibration, with ECE increasing by **13%** when UAT-LITE is applied. We hypothesize that in highly overparameterized models, stochastic perturbations introduced via Monte Carlo sampling may disrupt already well-formed attention patterns, leading to excessive variance propagation rather than meaningful uncertainty modeling. This observation suggests that uncertainty-weighted attention is most effective in the regime of small to mid-sized transformers, where model capacity and stochasticity appear to be better balanced.

Latency measurements further contextualize this behavior. While inference-time overhead remains moderate for mid-sized models (e.g., 7 ms  $\rightarrow$  39 ms for BERT-base), it increases substantially for larger architectures (26 ms  $\rightarrow$  134 ms for BERT-large), reinforcing the trade-off between calibration gains and computational cost.

## F Implementation and Reproducibility

This section characterizes the computational and implementation properties of UAT-LITE. We first analyze its asymptotic and practical computational complexity relative to standard transformer inference and ensemble-based uncertainty methods. We then quantify inference-time overhead introduced by Monte Carlo sampling and describe the experimental setup, hardware configuration, and reproducibility details required to replicate all reported results. Throughout, we emphasize that UAT-LITE operates strictly at *inference time* and does not modify pretrained parameters or training cost.

### F.1 Computational Complexity Analysis

UAT-LITE preserves the parameter count and training cost of the base transformer. All uncertainty-aware mechanisms operate strictly at inference time and do not introduce additional trainable parame-

Base Model	Domain	Dataset	Baseline ECE	+UAT-LITE ECE	Improvement
BERT-base	General	SQuAD	0.130	0.062	52% ↓
RoBERTa-base	General	MNLI	0.040	0.039	2% ↓
ClinicalBERT	Medical	MedQA	0.049	0.037	25% ↓
BiobERT	Biomedical	PubMedQA	0.120	0.072	40% ↓
SciBERT	Scientific	SQuAD	0.092	0.083	10% ↓
<b>Average</b>	—	—	0.086	0.059	<b>32% ↓</b>

Table 10: Cross-domain calibration performance across pretrained transformer backbones (single seed). Expected Calibration Error (ECE; lower is better) is reported for each model before and after applying UAT-LITE. Improvements are relative to each model’s baseline. Larger gains occur in tasks with pronounced epistemic uncertainty (e.g., SQuAD, PubMedQA), while models with strong baseline calibration (e.g., RoBERTa on MNLI) exhibit smaller improvements, indicating diminishing returns rather than method failure.

Model	Params	Baseline ECE	UAT-LITE ECE	Rel. Δ	Latency
BERT-tiny	4.4M	0.070	0.061	12% ↓	1 → 5
BERT-mini	11.2M	0.131	0.056	58% ↓	1 → 8
BERT-small	28.8M	0.095	0.081	15% ↓	1 → 9
BERT-base	109.5M	0.139	0.066	53% ↓	7 → 39
BERT-large	335.1M	0.152	0.172	13% ↑	26 → 134

Table 11: Effect of model capacity on calibration within the BERT family (single seed). Expected Calibration Error (ECE; lower is better) is reported before and after applying UAT-LITE. Uncertainty-aware attention yields the largest gains for small-to-mid-sized models, while very large models exhibit diminished or negative returns, indicating a capacity–stochasticity trade-off rather than a failure of the method. Latency reflects baseline → UAT-LITE inference time (ms).

ters or modify learned weights.

Additional computational cost arises solely from Monte Carlo (MC) sampling during inference:

- **Parameters:** identical to the base model (e.g., 109M for BERT-base)
- **Training cost:** unchanged
- **Calibration cost:** one scalar temperature per task (optional)
- **Inference cost:**  $M$  stochastic forward passes (typically  $M = 5$ )

From a complexity perspective, inference-time cost scales linearly with the number of Monte Carlo samples  $M$ . In contrast to ensemble-based approaches, which require training, storing, and evaluating multiple independent models, UAT-LITE incurs no additional training or memory overhead. As a result, its total computational footprint remains substantially lower than Deep Ensembles for comparable calibration gains.

## F.2 Inference-Time Overhead

While the previous subsection characterizes asymptotic complexity, we now report empirical

inference-time overhead under realistic deployment conditions.

At test time, UAT-LITE performs  $M$  stochastic forward passes through the same pretrained model. When executed sequentially, runtime increases approximately linearly with  $M$ . For BERT-base, this corresponds to a measured slowdown of approximately  $5.3 \times$  relative to deterministic inference when using  $M = 5$ .

Despite this overhead, inference-time cost remains practical for many deployment settings, particularly in scenarios where reliability and calibrated confidence are prioritized over raw throughput. Importantly, this cost is incurred only when uncertainty-aware inference is enabled and can be adjusted dynamically by reducing  $M$  for high-confidence inputs, as discussed in Section 7.

## F.3 Reproducible Experimental Setup

This subsection summarizes the experimental setup and implementation details necessary to reproduce our results. All experiments follow a consistent architecture, training configuration, and evaluation protocol across datasets.

### Model architecture.

- Base model: BERT-base-uncased
- Number of parameters: 110M
- Transformer layers: 12
- Hidden dimension: 768
- Attention heads: 12

#### Training hyperparameters.

- Optimizer: AdamW with standard settings
- Learning rate:  $2 \times 10^{-5}$
- Learning rate schedule: linear warmup for first 500 steps, followed by linear decay
- Batch size: 16
- Number of epochs: 3
- Weight decay: 0.01
- Gradient clipping: 1.0

#### UAT-LITE configuration.

- Inference via Monte Carlo sampling with  $M = 5$  stochastic forward passes
- Component-specific dropout rates:
  - Embedding layer: 0.1
  - Attention layers: 0.2
  - Feed-forward layers: 0.3
- Uncertainty weighting coefficient:  $\lambda = 0.5$  (set once on development data and held fixed across tasks)
- Sensitivity analysis for  $\lambda$  and  $M$  reported in §D.1

#### F.4 Hardware, Latency, and Code Availability

**Compute resources and latency measurement.** All experiments are conducted on a single NVIDIA A100 GPU (40GB). Unless otherwise stated, latency is measured as *end-to-end forward-pass wall-clock time per example*, averaged over 200 runs after 50 warm-up iterations. We use fixed sequence lengths (128 for SST-2 and MNLI; task-standard truncation for SQuAD answerability) and batch size 1.

For stochastic methods, latency is reported under the same Monte Carlo budget  $M$  used during evaluation. Reported slowdowns reflect the ratio between stochastic inference and deterministic baseline inference under identical conditions.

**Code availability.** To ensure reproducibility during the anonymous review process, we provide an anonymized repository containing the complete implementation, including training scripts, evaluation pipelines, and configuration files. All experiments are implemented using HuggingFace Transformers, PyTorch, and Python. The repository is available at: [https://github.com/eliashossain001/uq\\_decomposition/tree/main](https://github.com/eliashossain001/uq_decomposition/tree/main).

## G Supplementary Related Work

This section provides an extended discussion of prior work on calibration, uncertainty estimation, and uncertainty-aware Transformer modeling. Because the main paper focuses on method design and empirical evaluation rather than a comprehensive survey, we defer detailed comparisons to this supplementary section. We organize related work into three themes: (i) post-hoc calibration and ensemble-based uncertainty estimation, (ii) Bayesian Transformers and stochastic inference methods, and (iii) approaches that explicitly incorporate uncertainty into attention mechanisms. This structure clarifies how UAT-LITE differs from and complements existing techniques.

### G.1 Calibration and Uncertainty

Despite high predictive accuracy, modern neural networks are often poorly calibrated (Guo et al., 2017). Post-hoc calibration methods such as temperature scaling (Guo et al., 2017), Platt scaling (Platt et al., 1999), and histogram binning (Zadrozny and Elkan, 2001) adjust output confidence without altering internal representations. While simple and effective, these methods are limited by the quality of learned features and do not affect model reasoning.

Ensemble-based approaches improve calibration by averaging predictions from multiple models. Deep Ensembles (Lakshminarayanan et al., 2017) and snapshot ensembles (Huang et al., 2017) are among the strongest calibration baselines, but require training, storing, and evaluating multiple model replicas, resulting in substantial computational and memory overhead. More efficient approximations, such as ensembling pruned attention heads within a single Transformer (Gabetni et al., 2025), reduce cost but still rely on architectural modification or fused ensemble structures. Our work instead targets competitive calibration using inference-time stochasticity within a single pre-

trained model.

## G.2 Bayesian and Stochastic Methods

Bayesian neural networks provide principled uncertainty estimates by placing distributions over model parameters (MacKay, 1992; Neal, 2012). However, scalable approximations such as variational inference (Blundell et al., 2015; Louizos and Welling, 2017) and Laplace methods (Ritter et al., 2018) scale poorly to Transformer-sized models. Bayesian Transformer variants (Xue et al., 2021; Fan et al., 2020) further require architectural modification and retraining, limiting compatibility with pretrained backbones.

Several recent methods estimate uncertainty in weight space. Stochastic Weight Averaging and its Gaussian extension (SWAG) approximate posterior distributions during fine-tuning and improve uncertainty quality in NLI tasks (Talman et al., 2023). Parameter-efficient Bayesian adaptation methods such as C-LoRA (Rahmati et al., 2025) introduce latent variables within low-rank adapters, but require Bayesian fine-tuning and task-specific parameter updates. Other approaches improve uncertainty estimation through post-hoc output heads (Zabolotnyi et al., 2025) or uncertainty-aware loss reweighting during alignment (Wang et al., 2024). These methods primarily influence training dynamics or output distributions and do not modify internal Transformer computations at inference time.

Monte Carlo Dropout (Gal and Ghahramani, 2016) provides a lightweight alternative by approximating Bayesian inference through stochastic forward passes. Standard MC Dropout applies uniform stochasticity across layers and treats uncertainty only as an output-level signal. Our work builds on MC Dropout, but explicitly uses the resulting uncertainty to influence attention during inference.

## G.3 Uncertainty-Aware Attention

Calibration and uncertainty issues are particularly pronounced in Transformer-based models. Larger Transformers are often increasingly overconfident (Desai and Durrett, 2020), and semantic uncertainty plays a significant role in language understanding and generation (Kuhn et al., 2023). Most existing methods treat uncertainty as a post-hoc quantity, leaving attention patterns and internal representations unchanged.

Several approaches inject uncertainty directly into attention mechanisms. Bayesian Attention Be-

lief Networks (Zhang et al., 2021) model attention weights as latent random variables, while Sparse Gaussian Process Attention (Chen and Li, 2023) reformulates self-attention using kernel-based Gaussian process inference. Although principled, these methods require architectural changes and variational training, limiting their applicability to pre-trained models. Domain-specific uncertainty-aware Transformers, such as TUnA (Ko et al., 2024), introduce uncertainty primarily through output layers rather than through attention modulation itself.

Recent work explores efficient uncertainty mechanisms inspired by ensembles or parameter-efficient adaptation. Hydra Ensembles (Gabetni et al., 2025) approximate Deep Ensembles by fusing multiple attention heads, achieving competitive calibration with reduced cost. However, uncertainty arises from architectural fusion and remains an output-level aggregation. Similarly, C-LoRA (Rahmati et al., 2025) requires Bayesian fine-tuning to model uncertainty. Other methods leverage uncertainty for downstream decision-making, such as selective prediction (Vazhentsev et al., 2025), but do not affect internal attention computation.

**Positioning of UAT-LITE.** UAT-LITE integrates epistemic uncertainty into self-attention at *inference time*, without modifying pretrained weights, training objectives, or model architecture. Unlike post-hoc scalers (e.g., temperature scaling) that adjust confidence only at the output layer, our method uses uncertainty estimates to *modulate internal token interactions*, aiming to improve reliability under ambiguity, distribution shift, and selective decision-making. Importantly, UAT-LITE is *complementary* to post-hoc scaling: temperature scaling can be applied on top of our uncertainty-aware inference when the goal is to minimize in-domain calibration error while preserving uncertainty-aware internal computation.

## H AI Usage Statement

We used large language models as auxiliary tools during manuscript preparation. Claude was used for limited coding assistance, including refactoring and debugging support. ChatGPT was used for writing assistance, including grammar checking, spelling correction, and stylistic refinement. All core research contributions, including the scientific ideas, experimental design, implementation, empirical evaluation, analysis, and conclusions, were

developed by the authors. All results are based on our own experiments using publicly available datasets and verified code. No AI system was used to generate data, conduct experiments, or draw scientific conclusions.